DOI: 10.1002/chem.200903001

The "Flash" Method: A Shortcut for Producing the $Cs_x(W,Nb)_5O_{14}$ Structure

Anikó Simon and Evgenii V. Kondratenko*[a]

Complex mixed-metal oxides are fundamental materials for various applications since their physicochemical properties and structure can be tuned by altering metal content and oxygen stoichiometry. In particular, those of the formula of $(Mo,W)_a(V,Nb)_b(TeO_x,SbO_x)_cO_{14}$ ($a+b=5$, $x=1,2$, $0\leq c\leq 2$) are of essential interest in heterogeneous catalysis.[1] This system is attractive for converting cheap and in future longer available C_2–C_4 alkanes in natural gas to alkenes, nitriles, and oxygenates currently produced from oil-derived feeds.[2] These catalytic reactions are structure sensitive. The orthorhombic M1 phase, isostructural to the $Cs_x(W,Nb)_5O_{14}$ phase described first by Lundberg et al.,[3] is assumed to perform the alkane functionalization.[4] Preparing M1 structured materials usually involves several steps: a strict mixing order of all reagents, heating at ambient or elevated pressures, removal of solvents and drying, multiple calcinations in various atmospheres, and elution of by-phases (e.g., the hexagonal M2 phase[5]). Anyhow, the preparation of single-phase materials is still challenging, and often lacking in reproducibility.

Herein, we report on a shortcut method for preparation of the $Cs_x(W,Nb)_5O_{14}$ phase in only three simple steps. In contrast to the prior work of Shigapov et al.[6] aimed at creating simple metal oxides with a high surface areas, applying cellulose templates enabled us to produce an M1 structured single-phase material consisting of oxides of Mo, Nb, and Cs. We call this novel protocol the "flash" method. To demonstrate its benefits, we compared it to the standard slurry and hydrothermal routes for preparing the exemplary $CsMo_2Nb_3O_{14}$ compound. All materials were evaluated regarding their bulk crystallinity, elemental composition, surface morphology, and BET surface area, as well as preparation time and yield. Moreover, the cell parameters of the flash product were refined by the Rietveld method.

The preparation protocols are briefed below; further details are outlined in Scheme S1 in the Supporting Information. For each method, ammonium heptamolybdate, ammonium niobate oxalate, cesium nitrate, and deionized water were used unpurified. Firstly, the reagents were suspended in water and heated to reflux under stirring for 15 min.

For the hydrothermal route, the hot solution was filled into a teflon tube, sealed in a stainless steel autoclave, and heated at 458 K for 50 h, after which the autoclaves were quenched at room temperature. The resulting black suspension was decanted, washed, and dried at ambient pressure at 343 K for 18 h. The dark brown raw product was finally calcined in static air at 873 K for 6 h yielding 81.5 % of a light yellow solid (**HT873**). The calcination at 873 K was repeated owing to the poor crystallinity. The final product is later referred to as **HT873r**.

For the slurry route, the hot solution was transferred into a dish and evaporated at ambient pressure at 393 K. The bluish white residue was finally calcined at 873 K for 6 h to yield 98.0 % of the **SL873** product.

For the flash route, the solution was fully absorbed by cellulose (Carl Roth, 0.007 % ash). The impregnated wet fibers were directly placed in a red-hot furnace (873 K) and calcined in static air for 6 h, yielding 98.5 % of the **FL873** product.

We emphasize here, that the flash preparation takes the shortest time (in total less than seven hours to obtain the final product) and scored the highest overall yield (98.5 %). In contrast, the hydrothermal route claims the longest time (two days only to form the raw product) and resulted in the lowest yield (81.5 %). The preparation method also influences the BET surface area (Table 1). The low BET surface area of 3.0 m^2g^{-1} of the **SL873** material clearly stands out. The **HT873r** and **FL873** products have BET surface areas of 9.8 and 7.2 m^2g^{-1}, respectively.

SEM revealed that the different shapes and sizes of the crystallites explain the dissimilar BET surface areas. Figure 1 clearly evidences a porous surface of aggregated nanocrystallites in **HT873r**. On top, grooved rod-like needles

[a] Dipl. Chem. A. Simon, Dr. E. V. Kondratenko
Leibniz Institute for Catalysis at the University of Rostock
Albert-Einstein-Strasse 29A, 18059 Rostock (Germany)
Fax: (49) 381-1281-55290
E-mail: evgenii.kondratenko@catalysis.de

Supporting information for this article is available on the WWW under http://dx.doi.org/10.1002/chem.200903001.

Table 1. Elemental composition and BET values.

Sample	Elemental composition	BET area [m^2g^{-1}]
SL873	$Cs_{1.1\pm0.1}Mo_{1.73\pm0.03}Nb_{3.17\pm0.01}O_n$	3.0
HT873r	$Cs_{1.1\pm0.1}Mo_{1.32\pm0.05}Nb_{3.65\pm0.05}O_n$	9.8
FL873	$Cs_{1.2\pm0.1}Mo_{1.77\pm0.05}Nb_{3.1\pm0.1}O_n$	7.2

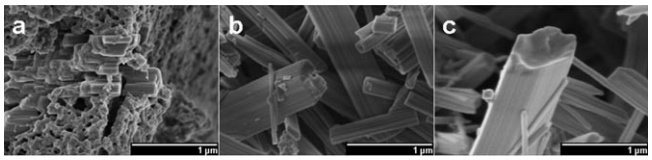

Figure 1. SEM micrographs of a) **HT873r**, b) **SL873** and c) **FL873** after calcination at 873 K. The scale bars are 1 μm.

are emerging out of the substrate. In view of that, **SL873** and **FL873** feature congeneric but full-grown grooved rods. Furthermore, no porous structures are spotted. Yet, **SL873** mainly formed to thick rods, while **FL873** mostly consists of thin needles, partly aggregated as seen from the SEM images in Figure S1 in the Supporting Information.

All products contain less Mo than expected from the formula of $CsMo_2Nb_3O_n$. **HT873r** lacks this element the most, resulting in the highest Nb/Mo ratio of 2.8 versus 1.8 in **SL873** and **FL873** (Table 1). The chemical composition of the last two materials is exactly equal. A minor loss of sublimating Mo oxide(s) during the calcination at 873 K cannot be ruled out. The leaching in the hydrothermal route may derive from the phase separation step. The removal of solvent, containing both reactants and fractions of the liquefied raw product, possibly leads to an elemental loss. However, a detailed investigation of the origins of the Mo leakage would exceed the scope of this communication.

In agreement with SEM, XRD analysis confirms a poor crystallinity of **HT873r** (Figure 2). The XRD diffractograms of **SL873** and **FL873** are characterized by well-resolved "finger-print" reflections of the $Cs_x(W,Nb)_5O_{14}$ phase in the 2θ region between 5 and 10°, as well as at 22.2° and 26.5°. The reflection at $2\theta = 22.2°$, observed in many Mo oxides of the layer-typed ReO_3 structure, is assigned to the interlayer distance d along the axis (001) equal to ≈ 4 Å. The distances determined for **HT873r**, **SL873**, and **FL873** are at 3.989, 3.999, and 4.001 Å, respectively, indicating a remarkably shorter interlayer distance in **HT873r**. This deviation may arise from the unequal chemical composition (Table 1).

Additional crystal phases other than $Cs_x(W,Nb)_5O_{14}$ were not observed within XRD resolution, though all materials seemingly contain moieties of X-ray amorphous phase(s). In order to obtain more information on the possible existence of X-ray amorphous individual oxides of Nb and Mo, the materials were analyzed by Raman spectroscopy. Figure 3 displays the Raman spectra of **FL873**, as well as of individual MoO_3 and Nb_2O_5. Comparing the band positions in the Raman spectrum of **FL873** with those in the spectra of the individual oxides, the presence of their amorphous nanocrystallites can be ruled out. It should be stressed here, that

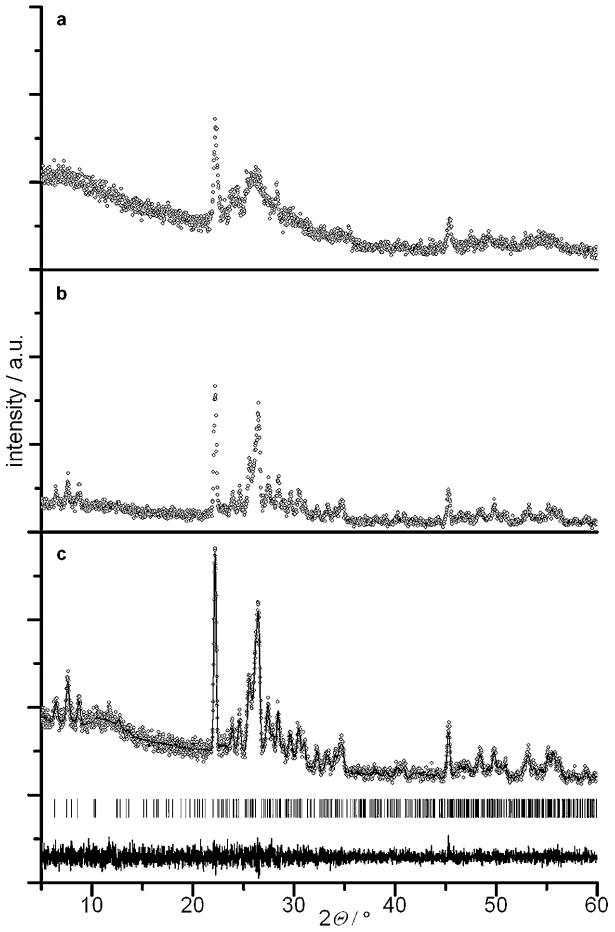

Figure 2. XRD patterns (circles) of a) **HT873r**, b) **SL873**, and c) **FL873** after calcination at 873 K. Bottom plot with calculated patterns (line), Bragg reflections (tick marks), and difference plot (beneath) from Rietveld refinement.

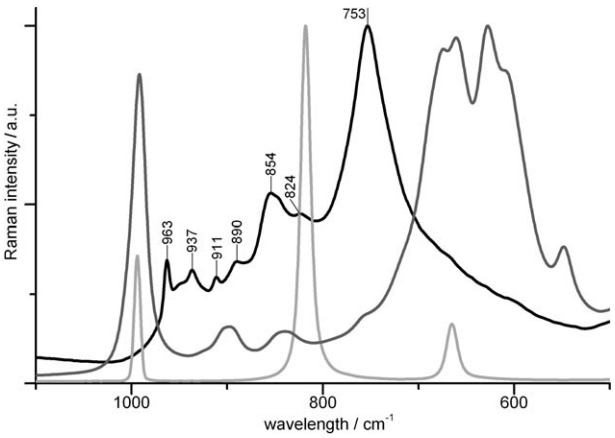

Figure 3. Raman spectra of **FL873** (black), MoO_3 (light gray), and Nb_2O_5 (dark gray).

both the Raman and XRD analysis proved the flash method to produce the best-crystallized material compared to the standard methods.

The orthorhombic structure of the flash product was simulated by refining the powder XRD data according to the least-squares Rietveld method using the GSAS/EXPGUI program.[7] Impurity reflections were not detected. The cell parameters of the estimated space group *Pba*2 are summarized in Table S1 in the Supporting Information. The fitting quality is reflected in the low overall R_F value of 3.31%. The final convergence resulted in an interlayer distance of 4.001 Å, in perfect match with the experimental data. Thus, judging from the difference plot between measured data and simulation (Figure 2c), the suggested structure of the **FL873** material turned out to be realistic.

In summary, the flash route is a hopeful advance in preparing $Cs_x(W,Nb)_5O_{14}$ structured materials. The application to the Mo-V-(Te/Sb)-Nb oxide system, which is catalytically active in the alkane oxyfunctionalization, is currently under progress. In a general sense, our novel method is appropriate for the bulk structuring of individual and mixed oxides of main and transition-metal groups and is to be employed for a broad variety of materials for applied chemistry. It excels with high-quality bulk crystallinity, a short preparation time, a high yield of crystalline product, and a minimum Mo leakage relative to the standard slurry and hydrothermal methods.

Experimental Section

The elemental composition was measured by X-ray fluorescence spectroscopy (XRF) on an Oxford ED-2000 spectrometer. Specific surface areas were computed from Kr physisorption at 120 K with single point BET procedure. A Stoe Stadi P transmission diffractometer with Ge-(111)-monochromatic $Cu_{K\alpha 1}$ radiation ($\lambda = 1.5406$ Å) was used for powder X-ray diffraction (XRD) study in the range of $5 \leq 2\theta \leq 60°$ with 0.05° steps. Rietveld refinement was performed using the GSAS/EXPGUI program package. Scanning electron microscopy (SEM) images were taken by a Hitachi S-4800 FEG at an acceleration voltage of 2.0 kV in the secondary electron (SE) mode. Raman spectra were collected using a Kaiser Optical Systems RXN1 equipped with a diode laser (785 nm) operating at a power level of 70 mW.

Acknowledgements

The assistance of the analytical department at LIKAT is appreciated: Dr. Radnik for XRF, Mr. Knoepke for Raman spectroscopy, and Mrs. Winkler for XRD and BET. Furthermore, we thank Mrs. Weinberg at FHI Berlin for SEM imaging. This work was partially supported by the DFG (Deutsche Forschungsgemeinschaft) within the collaborative research center (Sonderforschungsbereich) 546.

Keywords: cesium · molybdenum · niobium · polyoxometalates · synthetic methods

[1] a) Y. Uchida, G. Mestl, O. Ovsitser, J. Jäger, A. Blume, R. Schlögl, *J. Mol. Catal. A* **2002**, *187*, 247–257; b) J. Kunert, A. Drochner, J. Ott, H. Vogel, *Appl. Catal. A* **2004**, *269*, 53–61; c) I. E. Wachs, J.-M. Jehng, W. Ueda, *J. Phys. Chem. B* **2005**, *109*, 2275–2284; d) O. V. Safonova, B. Deniau, J.-M. M. Millet, *J. Phys. Chem. B* **2006**, *110*, 23962–23967.

[2] a) P. Botella, E. García-González, A. Dejoz, J. M. López Nieto, M. I. Vázquez, J. González-Calbet, *J. Catal.* **2004**, *225*, 428–438; b) T. Ushikubo, H. Nakamura, Y. Koyasu, S. Wajiki (Mitsubishi Kasei Corp.), US 5380933, **1995**; c) B. Solsona, F. Ivars, P. Concepción, J. M. López Nieto, *J. Catal.* **2007**, *250*, 128–138.

[3] M. Lundberg, M. Sundberg, *Ultramicroscopy* **1993**, *52*, 429–435.

[4] P. DeSanto, Jr., D. J. Buttrey, R. K. Grasselli, C. G. Lugmair, A. F. Volpe, B. H. Toby, T. Vogt, *Top. Catal.* **2003**, *23*, 23–38.

[5] E. García-González, J. M. López Nieto, P. Botella, J. M. González-Calbet, *Chem. Mater.* **2002**, *14*, 4416–4421.

[6] A. N. Shigapov, G. W. Graham, R. W. McCabe, H. K. Plummer, Jr., *Appl. Catal. A* **2001**, *210*, 287–300.

[7] a) A. C. Larson, R. B. Von Dreele, LANSCE MS-H805, LANL, **2000**; b) B. H. Toby, *J. Appl. Crystallogr.* **2001**, *34*, 210–221.

Received: October 30, 2009
Published online: January 11, 2010

